STUDY ON THE EXSOLUTION PHENOMENA OF PYROXENES

by

Yoshiaki YAMAGUCHI *

(with 4 Tables, 9 Figures and 4 Plates)

(Contribution from the Department of Geology and Mineralogy, Faculty of Science, Hokkaido University, No. 1322)

Abstract

For twenty pyroxene specimens in the $CaMgSi_2O_6$-$CaFeSi_2O_6$-$MgSiO_3$-$FeSiO_3$ system, the exsolution phenomena are examined by means of the X-ray single crystal diffraction in correlation with the optical investigation. Twelve Ca-rich clinopyroxene enclose the exsolution phases of both Ca-poor clinopyroxene and orthopyroxene, or of only Ca-poor clinopyroxene. Of all the Ca-rich clinopyroxenes from various igneous rocks, the members more Mg-rich than $Ca_{40}Mg_{42}Fe_{18}$ enclose (100) exsolution phases composed of both clinoenstatite-clinobronzite and orthoenstatite-orthobronzite, whereas the members more Mg-poor than this enclose (001) exsolution phases of clinohypersthene.

Four Ca-poor orthopyroxenes enclose (100) exsolution phases of Ca-rich clinopyroxenes, and three of these exsolved Ca-rich clinopyroxenes are twinned on the (100) as compositional plane and show apparently orthorhombic symmetry. A pigeonite encloses (001) exsolved augite, but a inverted pigeonite encloses exsolved augite that is randomly oriented with the host.

In most cases, exsolution and host pyroxene phases show one or two dimensional agreement not only in orientation but also in lattice dimension along their sharing axis or plane. So that most of the exsolved pyroxenes have been undergone lattice distortion, and do not show their intrinsic lattice dimensions. Exsolved clinoenstatites-clinobronzites and twinned Ca-rich clinopyroxenes as exsolution phases with apparently orthorhombic symmetry are metastable phases which have occurred under the lattice distortion in the early stage during the process of exsolution. In the later stage, they have grown to broad exsolution lamellae, resulting in the release of the lattice distortion and these metastable phases are convert into the stable phases.

* Present address: Department of Geology and Mineralogy, Kyoto University

Sometimes (100) diallage partings or strongly mosaic crystalline textures in some pyroxene crystals have been produced as the result of the release of the lattice distortion.

INTRODUCTION

The exsolution phenomena of pyroxene in igneous and metamorphic rocks have long been described by many petrologists as "lamellae", "pyroxene perthite", and "schiller" (BUCKING 1883, VOGT 1905, HARKER 1909 etc.). These phenomena were attributed by VOGT (1905) to the elimination of certain components in the silicate system on cooling.

HARKER (1935) classified two types of schiller structure in augite, i.e., one is diallage structure which shows schiller striations parallel to the (100) plane, and the other is salite structure which shows very minute striations parallel to the (001) plane.

HESS (1941) and POLDERVAART and HESS (1951) have studied the exsolution phenomena of pyroxene in plutonic rocks by means of the optical method. Based on the researches on the fractional crystallization of tholeiitic magma and the phase stability relation in the system $MgSiO_3$-$FeSiO_3$ established by BOWEN and SCHAIRER (1935), they demonstrated that the exsolution phenomena of pyroxene can be used as a geologic thermometer, and also that the types of pyroxene exsolved from the host are generally the same as those present as separate minerals in the same rock.

According to their studies there are five principal combinations with relative crystallographic relations in orientation between hosts and exsolution lamellae as follows.

> Augite with (100) hypersthene lamellae (*b*-and *c*-axes coincident), augite with (001) pigeonite lamellae (*a*-and *b*-axes coincident), augite with both (100) hypersthene and (001) pigeonite lamellae, hypersthene with (100) augite lamellae (*b*-and *c*-axes coincident), and pigeonite with (001) augite lamellae (*a*-and *b*-axes coincident). Some pigeonites from plutonic rocks include so-called "inverted pigeonites" which have been inverted from original pigeonites on subsequent cooling through the monoclinic – orthorhombic inversion temperature. "Inverted pigeonite" is a hypersthene enclosing coarse plates of augite elongated parallel to the (001) of original pigeonite before inversion. And from the same reason, many exsolved pigeonites in host augite itself have inverted to hypersthene.

BROWN (1957) has made a detailed study on the subsolidus exsolution of pyroxenes and their relation to the crystallization history of the Skaergaard

intrusion, arriving at the conclusions almost in agreement with HESS and POLDERVAART.

ITO and MORIMOTO (1958), and BOWN and GAY (1959, 1960) have studied the exsolution phenomena in pyroxenes by means of the X-ray single crystal method. Most of their results comfirmed the above interpretation obtained by the optical method. Recently, MORIMOTO and TOKONAMI (1969), in their study on the pigeonite from Moore County meteorite which shows oriented exsolution of two sets of augite lamellae parallel to the (001) and (100) of host pigeonite have found that the host and exsolved phases indicate two-dimensional agreement not only in orientations but also in lattice dimensions along their boundary planes, and therefore the exsolved phases do not show their intrinsic lattice dimensions. The difference between the two sets of augites in the lattice dimensions is attributed to lattice distortion during the exsolution.

On the other hand, BINNS et al. (1963) and BINNS (1965) have reported the existence of the (001) lamellae of exsolved clinohypersthenes in augites from two-pyroxene granulites from the results of the examination using the electron probe micro analyser and X-ray single crystal diffraction. BINNS (1965) explained that clinohypersthenes might have been separated from the host augite as the exsolution phases at temperature lower than granulite facies condition of metamorphism. Recently, YAMAGUCHI and TOMITA (1968, 1970) have found some clinoenstatites and clinobronzites as the exsolution phases almost completely sharing the (100) planes with the host diopsides from some ultra-mafic and mafic plutonic rocks. They considered that these exsolved pyroxene phases are the metastable phases which have been formed under the lattice distortion in the early stage during the process of exsolution of enstatite from the host diopside.

During the last 30 years, the opinions and interpretations given by HESS (1941), and POLDERVAART and HESS (1951) on the nature of the exsolution phenomena of pyroxene have been widely accepted. As mentioned above, however, recent findings, especially those of the exsolution of clino-hypersthenes (BINNS et al. 1963, BINNS 1965) or clino-bronzites and clinoenstatites (YAMAGUCHI and TOMITA, 1968, 1970) have shown that many problems on the nature and mechanism of exsolution phenomena in pyroxenes cannot be satisfactorily explained by HESS and POLDERVAART's interpretation.

In the present study, the author will study the exsolution phenomena of the pyroxenes in the system of $CaMgSi_2O_6$-$CaFeSi_2O_6$-$MgSiO_3$-$FeSiO_3$ from various kinds of rocks including ultra-mafic and mafic plutonic rocks from orogenic zone, the plutonic rocks from both tholeiitic and calc-alkalic series, and two-pyroxene granulite from regional metamorphic belt.

Table 1 Chemical compositions of pyroxene specimens

	C-1	C-2	C-3	C-4	C-5	C-6	C-7	C-8	C-9	C-10
SiO_2	54.59		51.91		51.45	51.57	51.22	51.27		51.7
TiO_2	0.32		0.19		0.89	0.12	0.35	0.46		0.2
Al_2O_3	1.48		4.59		4.02	3.42	2.79	1.87		1.2
Cr_2O_3	0.04		0.61		0.824	0.635		0.173		
Fe_2O_3			1.19		1.42	1.44	2.25	1.07		
FeO	2.48	1.55	2.20	3.54	2.52	2.27	4.67	9.70	10.70	11.4
MnO			0.15							
MgO	16.41	17.79	17.07	18.07	16.67	17.31	17.01	14.52	14.60	14.5
CaO	25.48	25.21	21.36	20.68	21.74	22.44	20.51	19.91	19.71	19.7
Na_2O					0.69	0.53	0.34	0.32		0.2
K_2O					0.00	0.00	tr.	0.00		
H_2O			0.34		0.23	0.22	0.38	0.38		
H_2O			0.08				0.09			
total	100.80		99.69		100.45	99.96	99.61	99.67		100.0

	C-11	C-12	C-13	C-14	R-1	R-2	R-3	R-4	P-1
SiO_2	51.12	50.73	50.93	50.52	54.39	54.83		54.0	53.59
TiO_2	0.45	0.90			0.11	0.23			
Al_2O_3	2.34	1.57	1.64	1.35	2.36	2.41		1.0	0.95
Cr_2O_3									
Fe_2O_3					2.10	2.34			
FeO	12.33	15.98	17.66	19.97	5.31	5.78	13.98	21.1	24.87
MnO									
MgO	14.76	12.84	13.49	7.54	33.79	33.21	29.17	23.1	17.33
CaO	18.63	17.51	16.59	19.26	1.35	1.35	1.43	2.0	4.25
Na_2O	0.34	0.27		0.44	0.09	0.13			
K_2O					0.00	0.00			
H_2O					0.15	0.32			
H_2O					0.01	0.05			
total	99.97	99.80	100.31	99.09	99.66	100.65		101.2	100.99

C-2, 3, 4, 7 and 9; analyst, Y. Yamaguchi.
C-1 and 10; analyst, M. Komatsu.
C-5, 6 and 8; analyst, M. Nochi.
R-1, 2 and 3; analyst, Y. Yamaguchi.
C-11, 12, 13 and 14, R-4, P-1; analyst, M. Komatsu.

SPECIMEN DESCRIPTION

The present study has been made on twenty pyroxene specimens, of which seventeen are newly examined, and three have already been reported by YAMAGUCHI and TOMITA (1968, 1970). The chemical compositions of these pyroxenes are shown in Tables 1 and 2, and are plotted in the diagram of $CaMgSi_2O_6$-$CaFeSi_2O_6$-$MgSiO_3$-$FeSiO_6$ (Fig. 1).

For each specimen the exsolution texture was examined under the microscope in thin section. The shape, orientation, extinction angle and other characteristic features of the exsolved phases are given as follows;

C-1 Diopside from peridotite in Ôgawara ultra-mafic body from Sambagawa metamorphic belt, Nagano Prefecture, Japan. The crystal is elongated parallel to the *c*-axis and displays strong bending of the (100) plane about the *b*-axis.

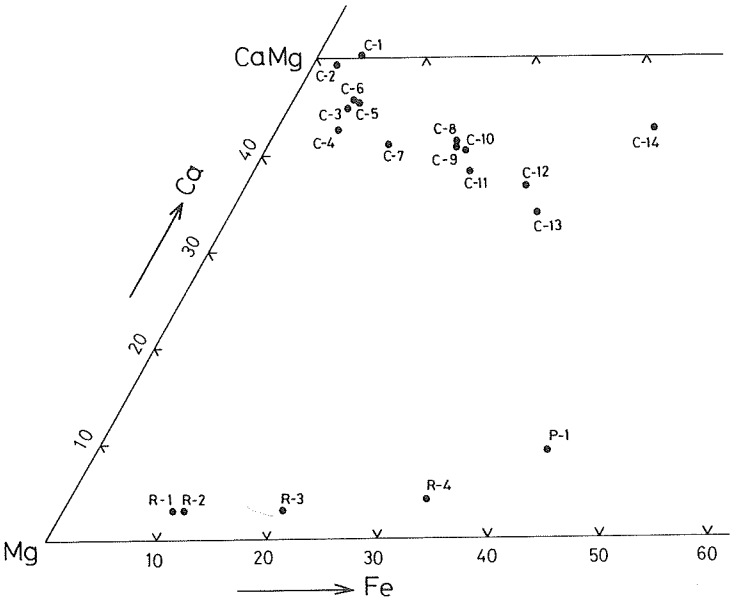

Fig. 1 Compositions of pyroxene specimens plotted in $CaMgSi_2O_6$-$CaFeSi_2O_6$-$MgSiO_3$-$FeSiO_3$ diagram.

Table 2 Compositions and optical properties of pyroxene specimens.

Specimen	Composition			Optical properties	
	Ca	Mg	Fe	γ	2V
1 C-1 diopside	51	45	4	1.698	60°(+)
2 C-2 diopside	49	49	2	1.694	58°(+)
3 C-3 diopside	45	50	5	1.701	59°(+)
4 C-4 diopside	42	52	6	1.702	55°(+)
5 C-5 diopside	45	49	6	1.700	
6 C-6 diopside	46	49	5	1.700	60°(+)
7 C-7 augite	41	48	11	1.709	55°(+)
8 C-8 augite	41	42	17	1.713	50°(+)
9 C-9 augite	40	42	18	1.716	50°(+)
10 C-10 augite	41	41	18	1.717	45°(+)
11 C-11 augite	38	42	20	1.718	47°(+)
12 C-12 augite	37	37	26	1.720	51°(+)
13 C-13 augite	34	38	28	1.728	41°(+)
14 C-14 ferroaugite	43	23	34	1.732	57°(+)
15 R-1 bronzite	3	87	10	1.681	102°(−)
16 R-2 bronzite	3	86	11	1.682	98°(−)
17 R-3 bronzite	3	77	20	1.689	78°(−)
18 R-4 hypersthene	4	64	32	1.701	63°(−)
19 P-1 pigeonite	9	50	41	1.721	14°(−)
20 P-2 inverted pigeonite				1.721	55°(−)

The twin lamellae (5-40μ in width) parallel to the (001) plane are observed, and the (001) partings are well-developed along the boundary surface (Plate 1, Fig. 1). Ca-poor pyroxene is absent in the host rock.

C-2 Diopside from the contact skarn, Hôshu Mine, Korea. The twin lamellae (10-40μ in width) parallel to the (001) and the (001) partings are well-developed as in C-1 diopside (Plate 1, Fig. 2).

C-3 and C-4 Diopsides (from Horoman ultra-mafic body), *C-5 and C-6 Diopsides* (from Pankenushi ultra-mafic body) in peridotites from the Hidaka metamorphic belt, Hokkaido, Japan. They show exsolution lamellae (1-10μ in width) parallel to the (100) plane, and the (100) diallage partings are poorly developed (Plate 1, Fig. 3). These exsolution lamellae display wavy extinction, and their extinction angles (c^z) vary in the range between 0° and approximately 30°. Each diopside coexists with Ca-poor orthopyroxene (En_{91} -En_{85}) in the host rock.

C-7 Augite (from olivine-gabbro, Opirarukaomappu area, Horoman), *C-8 Augite* (from norite, Pankenushi area) and *C-9 Augite* (from gabbroic rock in Horoman Ultra-mafic body) from the Hidaka metamorphic belt, Hokkaido, Japan. The crystals enclose broad exsolution lamellae parallel to the (100), and the (100) diallage partings are well-developed (Plate 1, Fig. 4 and Plate 2, Fig. 1). Sometimes the exsolved lamellae are grown into broad lenticular blebs, 20-30μ in width, along these partings. The exsolution lamellae and blebs display strong wavy extinction. Their extinction angles (c^z) vary in the range between 0° and 34°. C-8 Augite coexists with bronzite in the host rock, but in the case of C-7 and C-9 Diopsides Ca-poor pyroxene is absent in each host rock.

C-10 Augite in gabbro from Koyama calc-alkalic intrusion, Susa, Yamaguchi Prefecture, Japan. The crystal shows narrow streaks of the exsolution lamellae (1-2μ in width) parallel to the (001) under the open nicols. They are more clearly seen under the crossed nicols because of the slight difference in extinction angle between the host augite and the exsolution lamellae (Plate 2, Fig. 2). The Z-direction of the lamellae makes an angle 36° with the *c*-axis of the host augite. Sometimes the augite crystal are twinned on the (100) plane, and show "herring bone" structure. The coexisting Ca-poor pyroxene in the host rock is R-4 bronzite.

C-11 Augite in gabbro from Sano river calc-alkalic igneous complex, Kamisano, Yamanashi Prefecture, Japan. The orientation relations and other characteristic features of the exsolution lamellae are almost the same as C-11 augite. However, this (001) lamellae are too fine (less than 1μ in width) to measure the extinction angle. The coexisting Ca-poor pyroxene in the host rock is bronzite (En_{29}).

C-12 Augite from diorite, Loundoun Co., Virginia, U.S.A. The crystal has

exsolution lamellae (1-2μ in width) parallel to the (001) as well as C-10 and C-11 augites. Sometimes "herring bone" structure is seen. Inverted pigeonite, coexists in the host rock.

C-13 Augite from tholeiitic dolerite, Semi, Yamagata Prefecture, Japan. The crystal is elongated along *c*-axis, and sometimes (001) partings are seen (Plate 2, Fig. 3). Exsolution lamellae can not be observed in any orientation. Uninverted pigeonite with no exsolution lamellae coexists in the host rock.

C-14 Ferroaugitee in two-pyroxene granulite, from Vest Agder, Norway. The crystal has two kinds of exsolution lamellae; one is parallel to the (100), and the other is parallel to the (001) (Plate 2, Fig. 4). The (100) partings are well-developed along the boundary plane between the (100) lamellae and the host crystal. The (100) lamellae display almost straight extinction with the *c*-axis of host augite. The Z-direction of the (001) lamellae makes angle 34° with the c-axis of the host augite. The coexisting Ca-poor pyroxene is represented by ferrohypersthene in the host rock.

R-1 Bronzite from peridotite in the Horoman ultra-basic body from the Hidaka metamorphic belt, Hokkaido, Japan. The crystal shows fine lamellae structure due to the presence of very fine lamellae parallel to the (100), which form regular sheets, 1-2μ in width (Plate 3, Fig. 1). These (100) lamellae show oblique extinction of 22° with the (100) of the host bronzite. The birefringence of these (100) lamellae is exceedingly low, and their interference color is nealy the same as that of the host. Coexisting Ca-rich pyroxene in the host rock is diopside, which has chemical composition almost similar to the C-3 and C-6 diopsides in the present study.

R-2 Bronzite in pyroxene-rich segregation band of peridotite in ultra-basic body from the Hidaka metamorphic belt, Hokkaido, Japan. The crystal has the (100) lamellae as R-1 bronzite but these (100) lamellae are 3 to 5 times as broad as the latter (Plate 3, Fig. 2). They show oblique extinction of 37° with the (100) of the host, and the interference color is much higher than that of the fine lamellae in R-1 bronzite on the (010). This bronzite coexists with the diopside which has a similar chemical composition to that of C-3 or C-6' diopside in the host rock.

R-3 Bronzite from norite in Horokanai ultra-basic body from the Kamuikotan metamorphic belt, Hokkaido, Japan. The crystal has fine (100) lamellae (1-3μ in width) with the same characteristic features as those in R-1 bronzite. These fine lamellae are frequently grown to broad plates, 3-10μ in width, but both the fine lamellae and the broad plates have similar optical properties. Diopside (Wo_{49} En_{42} Es_9) coexists in the host rock.

R-4 Bronzite from gabbro of Koyama calc-alkalic intrusion, Susa, Yamaguchi Prefecture, Japan. The crystal displays striated structure due to the

presence of exceedingly fine lamellae parallel to the (100). The interference color of these fine lamellae is as low as that of the fine lamellae in R-1 bronzite. They are too narrow to determine the extinction angle. The areas of the crystal without these fine lamellae show somewhat incomplete extinction, and unnumerable faint streaks are seen parallel to the (100). This extinction anomaly suggests the presence of very fine lamellae in sub-microscopic domain size parallel to the (100). Coexisting Ca-rich pyroxene in the host rock is C-10 augite in this study.

P-1 Pigeonite and *P-2 Inverted Pigeonite* from gabbro of Koyama calc-alkalic intrusion, Susa, Yamaguchi Prefecture Japan. Most of pigeonites in the host rock have been inverted to hypersthene. P-1 pigeonite crystal preserves the original monoclinic crystal structure, which has exsolution lamellae (2-5μ in width) parallel to the (001). These (001) lamellae are 2-3 times as broad as the (001) lamellae in C-10 augite. Their extinction angle is slightly smaller than that of the host pigeonite (about 3°). This uninverted pigeonite exists in an area which is prevented from the inversion to hypersthene within the single crystal of inverted pigeonite (Plate 3, Fig. 3). In this crystal hypersthene and uninverted pigeonite share the (100) of each other.

P-2 inverted pigeonite has been completely inverted to hypersthene from original pigeonite and the crystal does not include uninverted pigeonite. Inverted pigeonite has broad exsolution lamellae parallel to the (001) of the original pigeonite. These (001) lamellae are 2-3 times broader than those in uninverted pigeonite, and sometimes they develop to large blebs or patchs (10-20μ in width), elongated parallel to the (001) of the original pigeonite. Sometimes, inverted pigeonite are twinned on (100), and shows "herring-bone" structure (Plate 3, Fig. 4). Coexisting Ca-rich pyroxene in the host rock is C-10 augite in this study.

EXPERIMENTALS

The crystals for X-ray investigation must be selected in correlation with the optical observation. For this reason, well-shaped (010) or (110) crystal flakes which show the exsolution texture under the microscope were used throughout this study.

The *hk1** (k=0,1,2), and *hk0** or *0k1** precession photographs were obtained for each specimen selected as mentioned above by using Mo-Kα radiation. Since all the exsolved phases, except the one in P-2 inverted pigeonite, share the *b*-axis with each host pyroxene, extra spots by exsolution phases appear in each *h01** photograph besides those by host pyroxene phases.

They are always arranged on the symmetrical positions related to the symmetry elements of the host pyroxene phases.

Following combinations of host and exsolved pyroxene phases are found in this examination;

Exsolution phase in Ca-rich clinopyroxene:

Clinopyroxene with space group $P2_1/c$ shares completely or almost completely the (100) or the (001) with the host. Orthopyroxene with space group Pbca shares the (100) with the host.

Exsolution phase in Ca-poor orthopyroxenes:

Clinopyroxene with space group $C2/c$ shares the (100) with the host.

Twinned clinopyroxene with space group $C2/c$ shares the (100) with the host.

Exsolution phase in Ca-poor clinopyroxene:

Clinopyroxene with space group $C2/c$ shares almost completely the (001) with the host.

It was noticed in many crystals that the host and exsolved phases have not only one or two crystallographic axes in common but also same lattice dimensions as will be mentioned in next chapter (Table 3).

RESULTS OF LATTICE ANALYSES

1. Ca-rich pyroxenes

C-1 and C-2 Diopsides These crystals present the patterns of a single twinning on the (001) as the compositional plane. Extra spots by any exsolution phase can not be observed.

C-3, C-4 and C-6 Diopsides All the crystals in which exsolution lamellae can be seen under the microscope display strong asterisms of X-ray diffraction spots (Plate 4, Fig. 1). The exsolution lamellae are composed of different two lattices, a clinopyroxene with space group $P2_1/c$, and an orthopyroxene with space group *Pbca* (Fig. 2 and Plate 4, Fig. 2). The former shared almost completely the (100) with the host diopside (two planes make about 20'), the later shares the (100) with the host diopside.

C-5 Diopside The crystal in which the broad exsolution lamellae can be seen under the microscope displays also strong asterism of X-ray diffraction spots. There is only an orthopyroxene with space group *Pbca* as an exsolution phase, (Fig. 2). On the other hand, small crystal piece (0.07 mm in width) without the exsolution lamellae does not displays such asterism of diffraction spots as above. Although the crystal is optically homogeneous under the microscope, extra spots are observed in addition to those by the host diopside

Table 3 Lattice dimensions and space group of both host and exsolved pyroxenes.

	Space group	a_0 (Å)	b_0 (Å)	c_0 (Å)	β
C-1	C2/c (host)	9.746	8.924	5.252	105°46′
C-2	C2/c (host)	9.747	8.920	5.256	105°55′
C-3	C2/c (host)	9.717	8.889	5.250	106°07′
	$P2_1/c$ (100)	9.59	8.82	5.20	108°38′
	Pbca (100)	18.18	8.82	5.20	
C-4	C2/c (host)	9.73	8.89	5.26	106°05′
	$P2_1/c$ (100)	9.58		5.21	108°33′
	Pbca (100)	18.17		5.21	
C-5	C2/c (host)	9.72	8 89	5.25	106°09′
	$P2_1/c$ (100)	9.09	8.88	5.18	108°39′
	Pbca (100)	18.18	8.83	5.20	
C-6	C2/c (host)	9.75	8.89	5.26	106°07′
	$P2_1/c$ (100)	9.60	8.84	5.21	108°33′
	Pbca (100)	18.21	8.84	5.21	
C-7	C2/c (host)	9.748	8 906	5.261	106°00′
	$P2_1/c$ (100)	9.62	8.88	5.23	108°26′
	Pbca (100)	18.26	8.88	5.23	
C-8	C2/c (host)	9.76	8.92	5.26	106°00′
	$P2_1/c$ (100)	9.64	8 89	5.23	108°33′
	Pbca (100)	18.27	8.89	5.23	
C-9	C2/c (host)		8.91	5.27	
	$P2_1/c$ (100)	9.65	8.88	5.23	108°40′
	Pbca (100)	18.29	8.88	5.23	
C-10	C2/c (host)	9.76	8.93	5.26	106°01′
	$P2_1/c$ (001)	9.67	8.93	5.22	108°45′
	Pbca (100)	18.29		5.21	
C-11	C2/c (host)	9.76	8.93	5.26	105°56′
	$P2_1/c$ (001)	9.76	8 93	5.22	108°50′
C-12	C2/c (host)	9.77	8.93	5.26	105°54′
	$P2_1/c$ (001)	9.77	8.93	5.22	108°53′
C-13	C2/c (host)	9.76	8.95	5.26	106°16′
	$P2_1/c$ (001)	9.76	8.95	5.23	108°44′
C-14	C2/c (host)	9.79	8.97	5.26	105°38′
	$P2_1/c$ (001)	9.74	8.97	5.23	108°43′
	$P2_1/c$ (100)	9.69	8.97	5.24	108°34′
	Pbca (100)	18.37	8.97	5.24	
R-1	Pbca (host)	18.235	8.805	5.183	
	C2/c (100)	9.34	8.81	5.21	
R-2	Pbca (host)	18.254	8.814	5.194	
	C2/c (100)	9.38	8.81	5.23	
R-3	Pbca (host)	18.268	8.849	5.204	
	C2/c (100)	9.35	8.85	5.25	
R-4	Pbca (host)	18.29	8.88	5.22	
	C2/c (100)	9.38	8.88	5.22	
P-1	$P2_1/c$ (host)	9.17	8.94	5.23	108°36′
	Pbca (100)	18.34		5.23	
	C2/c (001)	9.39	8.93	5.26	105°50′
P-2	Pbca (host)	18.33	8.93	5.23	
	C2/c (100)	9.39	8.93	5.25	

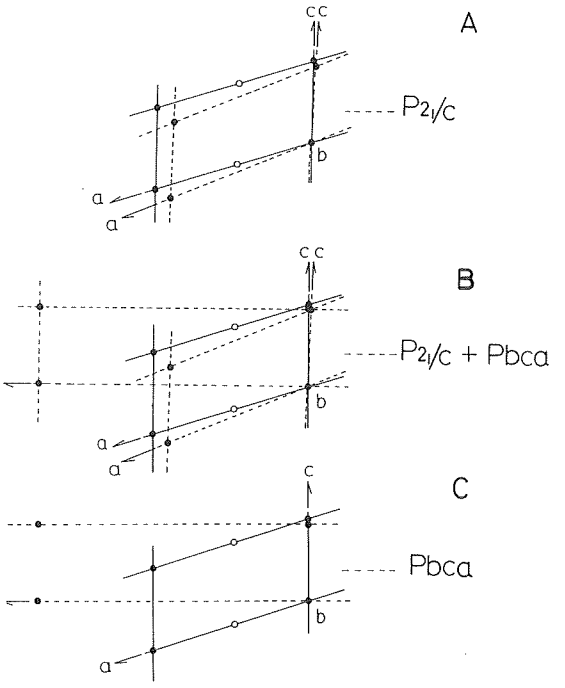

Fig. 2 Crystallographic orientations of the (100) exsolution phases in Ca-rich clinopyroxenes.
Solid line; host Dotted line; exsolution
A C-5 diopside crystal without exsolution lamellae
B C-3, 4 and 6 diopside
C C-5 diopside

phase, indicating the presence of a clinopyroxene with space group $P2_1/c$ as an exsolved phase (Fig. 2 and Plate 4, Fig. 3). The exsolved clinopyroxene in sub-microscopic domain size has slightly larger lattice dimension *b* and slightly smaller lattice dimention *c* than those of exsolved clinopyroxenes in C-3, C-4 and C-6 diopsides.

C-7, C-8 and C-9 Augites Exsolution lamellae in these three augites are composed of two kinds of pyroxenes, i.e., a clinopyroxene with space group $P2_1/c$ and an orthopyroxene with space group *Pbca*. The former shares almost completely the (100) with the host diopside and the latter shares the (100) with the host diopside as well as those in C-3 – C-6 diopsides. Although the (100) diallage partings are well-developed and strong mosaic crystalline texture is observed under the microscope in these augite crystals, asterism in diffraction spots as seen in the case of C-3 – C-6 diopsides is never observed in X-ray photographs.

C-10 Augite The diffraction patterns show the presence of two kinds of exsolution phases (Plate 4, Fig. 4); a clinopyroxene with space group $P2_1/c$, which shares almost completely the (001) with the host augite (two planes make an angle of about 14'), and an orthopyroxene with space group *Pbca*, which share the (100) with the host augite. The exsolved two phases and the host augite have identical *b*-axis not only in its orientation but also in its lattice dimension. Therefore the exsolved two phases may have been undergone one dimensional lattice distortion along *b*-axis.

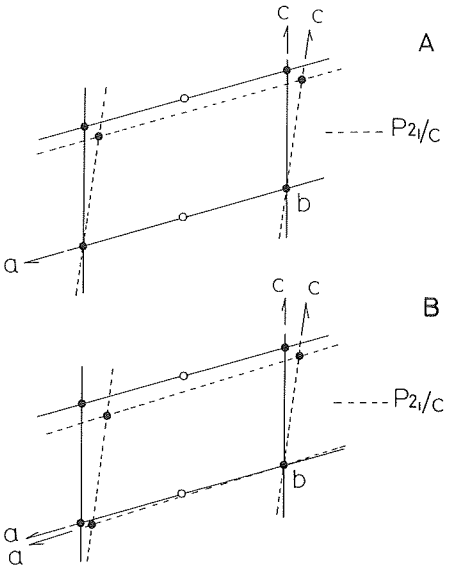

Fig. 3 Crystallographic orientations of the (001) exsolution phases in Ca-rich clinopyroxene.
Solid line; host Dotted line; exsolution
A C-11, 12 and 13 augites
B C-10 augite and C-14 ferroaugite

C-11 and C-12 Augites The (001) exsolution lamellae are composed of clino pyroxene with a space group $P2_1/c$. However, the exsolved clinopyroxene and the host augite share the (001), and they indicate two dimensional agreement not only in orientation but also in lattice dimention along this (001) boundary plane (Fig. 3). Therefore exsolved clinopyroxene may have been undergone two dimensional lattice distortion along the (001).

C-13 Augite Though the crystal is optically homogeneous under the microscope, extra spots are observed, indicating the presence of exsolved clinopyroxene with space group $P2_1/c$. The exsolved clinopyroxene in submicroscopic domain size shows two dimensional lattice distortion along the (001).

C-14 Ferroaugite The (001) exsolution lamellae are composed of clinopyroxene with space group $P2_1/c$, which shares almost completely the (001) with the host ferroaugite in the same way as that in C-10 augite (Fig. 4). The

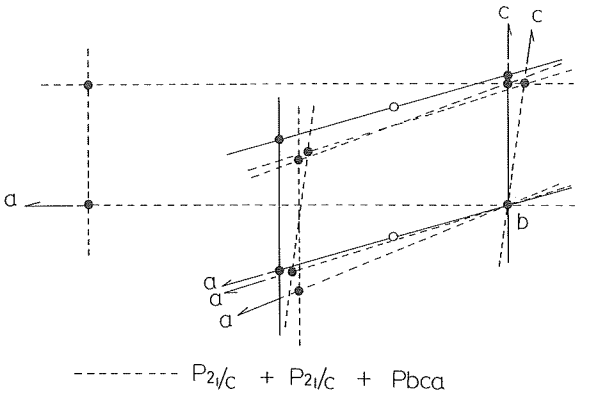

Fig. 4 Crystallographic orientations of both (100) and (001) exsolution phases in C-14 ferroaugite.
Solid line; host Dotted line; exsolution

(100) exsolution lamellae are composed of different two pyroxene phases; a clinopyroxene with space group $P2_1/c$, and an orthopyroxene with space group *Pbca*. These two pyroxene phases share the (100) with the host augite and they indicate one- dimensional agreement with the host augite in lattice dimension along their common *b*-axes. So that these exsolved two pyroxene phases show one- dimensional lattice distortion along their *b*-axis.

2. Ca-poor pyroxenes

R-1 and R-3 Bronzites The extra spots by exsolution phases are arranged in the symmetrical position related to the apparently orthorhombic symmetry elements (Fig. 5 and Plate 5, Fig. 1). It is difficult to determine strictly its space group because of the scarcity of these extra spots. Their apparent *a*, *b* and *c*-axes are coincident with the *a*, *b* and *c*-axes of the host bronzite respectively. The apparently orthorhombic phase may be presumably twinned clinopyroxene with space group $C2/c$ (Fig. 6). Since exsolved clinopyroxene shows equal lattice angle β in both settings of *C*-lattice and *I*-lattice, and it is twinned on (100) as the compositional plane, the arrangement of the lattice points shows apparent orthorhombic symmetry.

R-2 Bronzite The (100) exsolution lamellae are clinopyroxene with space group $C2/c$. The diffraction patterns do not show such twinning as the exsolution phase in C-2 and C-3 bronzites (Fig. 6 and Plate 5, Fig. 2). The exsolution and host phases share the (100), and further, the lattice dimensions *b* of the both phases are identical.

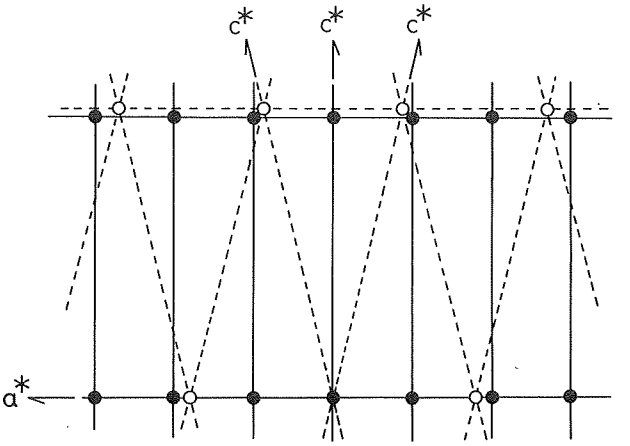

Fig. 5 Reciplocal lattices of both (100) exsolution phase and host in R-1 bronzite
Solid line; host Dotted line; exsolution

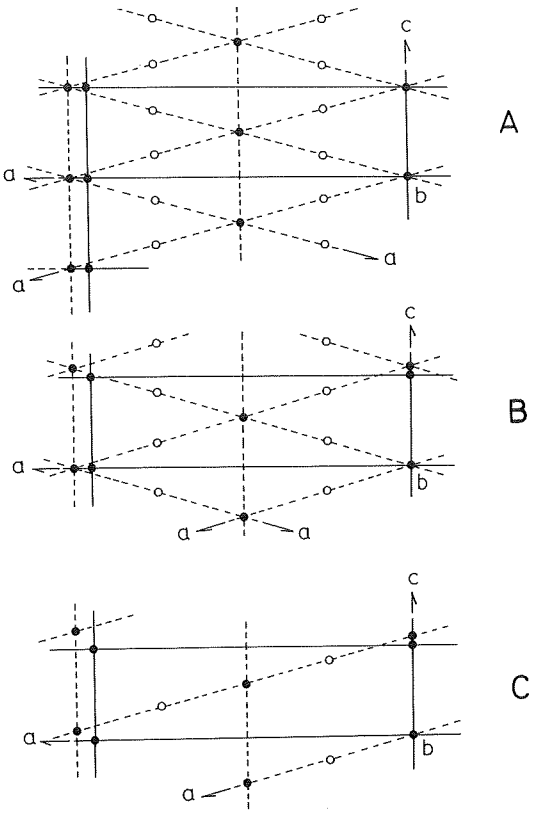

Fig. 6 Crystallographic orientations of the (100) exsolution phases in Ca-poor orthopyroxene.
Solid line; host Dotted line; exsolution
A Exsolved twinned clinopyroxene in R-4 hypersthene
B Exsolved twinned clinopyroxene in R-1 and R-3 bronzite
C Exsolved clinopyroxene in R-2 bronzite

R-4 Bronzite The (100) exsolution phase is twinned clinopyroxene with such apparently orthorhombic symmetry as those in R-1 and R-3 bronzites. However, this twinned clinopyroxene and the host bronzite share the (100) not only in orientation but also in lattice dimension (Fig. 6). Therefore this exsolved phase indicates two-dimensional lattice distortion.

P-1 Pigeonite Host pyroxene is composed of two kinds of pyroxene; a clinopyroxene with space group $P2_1/c$, and an orthopyroxene with space group

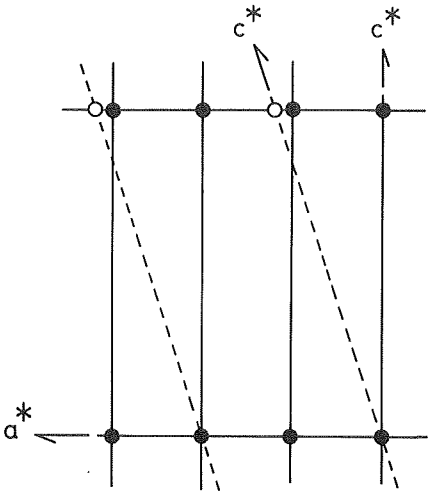

Fig. 7 Reciprocal lattices of host pyroxene phases in P-1 pigeonite.
Solid line; orthopyroxene with space group *Pbca*
Dotted line; clinopyroxene with space group $P2_1/c$

Pbca. They share the (100) in common (Fig. 7). The (001) exsolution lamellae are composed of clino-pyroxene with space group $C2/c$, which shares almost completely the (001) with the host pigeonite.

P-2 Inverted Pigeonite Extra spots are randomly arranged in the X-ray photographs, but no crystallographic relation in orientation between the exsolution and the host hypersthene is found (Plate 5, Fig. 3).

CHEMICAL COMPOSITION OF THE EXSOLUTION PHASES

Chemical analyses of exsolution lamellae are made for some pyroxene specimens by using the electron prove micro-analyser. The results are presented in Table 4, Fig. 8 and Fig. 9.

The (100) lamellae in Ca-rich clinopyroxene have very low Ca content, indicating that they belong to the members of the enstatite – ferrosilite series.

Table 4 Chemical compositions of exsolution lamellae

	1	2	3	4	5	6
SiO_2	54.39	53.83	51.65	51.62	53.72	52.27
Al_2O_3	3.50	n.d.	n.d.	n.d.	n.d.	0.76
FeO	6.65	16.30	18.52	3.13	4.12	26.53
MgO	33.17	23.63	22.40	17.01	16.83	18.21
CaO	0.66	2.21	1.98	23.06	23.85	1.06
Total	98.37	95.98	94.55	94.82	98.52	98.83
Mg	89	69	67	48	46	54
Fe	10	27	29	5	7	44
Ca	1	4	4	47	47	2

1: (100) lamellae in C-5 Diopside.
2: (100) lamellae in C-7 Augite.
3: (100) lamellae in C-8 Augite.
4: (100) lamellae in R-2 Bronzite.
5: (100) lamellae in R-3 Bronzite.
6: Host pyroxene in P-1 Pigeonite.

(Analyst M. Komatsu)

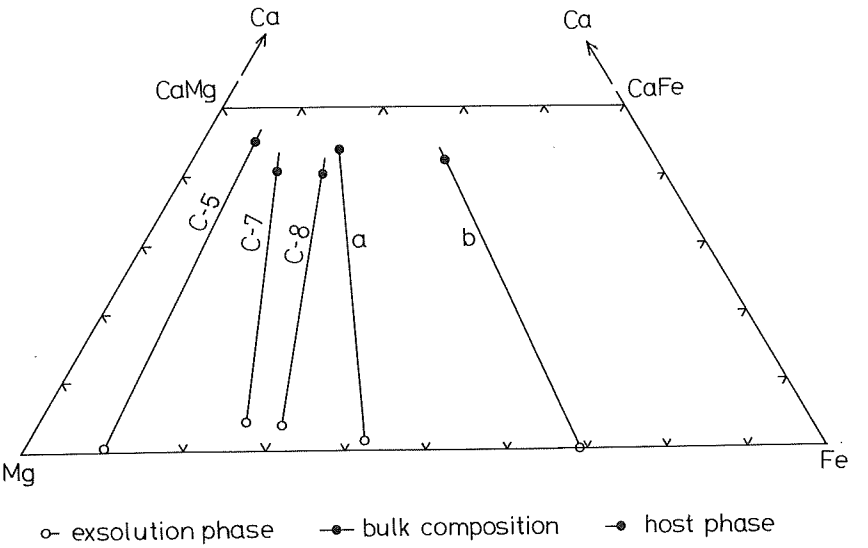

Fig. 8 Compositions of exsolution lamellae in some Ca-rich clinopyroxenes plotted in $CaMgSi_2O_6$-$CaFeSi_2O_6$-$MgSiO_3$-$FeSiO_3$ diagram.
a; augite from the Bushveld intrusion (Boyd and Brown 1969)
b; ferroaugite from the Willyama metamorphic Complex (Binns 1965)

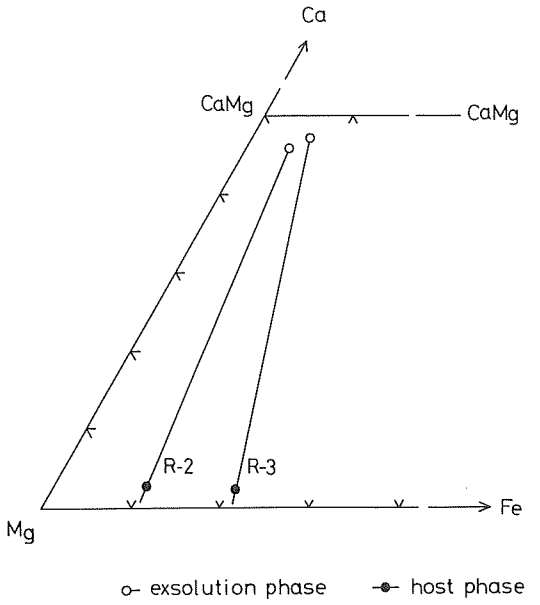

Fig. 9 Compositions of exsolution lamellae in some Ca-poor orthopyroxenes plotted in $CaMgSi_2O_6$-$CaFeSi_2O_6$-$MgSiO_3$-$FeSiO_3$ diagram.

Therefore, the exsolved clinopyroxenes with space group $P2_1/c$ in Ca-rich clinopyroxenes should be the members in clinoenstatite – clinoferrosilite series.

The chemical compositions of the (100) lamellae in Ca-poor orthopyroxene are high in CaO, indicating that they belong to Ca-rich clinopyroxene. It is worthy of note that in spite of their apparent orthorhombic symmetry caused by lattice distortion as mentioned in the foregoing chapter, these (100) exsolution phases have the chemical composition corresponding to Ca-rich clinopyroxene. Since host phase in P-1 pigeonite crystal has extremely low Ca content, pigeonite host should have changed its chemical composition to clinohypersthene in the process of exsolution of Ca-rich clinopyroxene.

DISCUSSIONS

Ca-rich clinopyroxenes of many basic plutonic rocks, especially those of tholeiitic affinities enclose the (100) or (001) exsolution lamellae. HESS (1941), and POLDERVAART and HESS (1951) mentioned that the (100) and (001) exsolution are orthopyroxene and pigeonite, respectively.

According to their interpretation, the Fe-poor clinopyroxenes crystallized

below the pigeonite – orthopyroxene inversion enclose the (100) orthopyroxene lamellae whereas clinopyroxenes more Fe-rich than approximately Ca_{41} Mg_{44} Fe_{15} crystallized above the pigeonite – orthopyroxene inversion temperature exsolve the (001) pigeonite lamellae, which are inverted in many cases to orthopyroxene on subsequent cooling.

1. Eight Ca-rich clinopyroxene specimens studied here enclose (100) lamellae. The (100) lamellae in seven of them are composed of two kinds of Ca-poor pyroxene, i.e., one is clinoenstatite – clinohypersthene and the other is orthoenstatite – hypersthene, but small crystal piece (from C-5 diopside) free from visible exsolution lamellae has an exsolution phase of only clinoenstatite in submicroscopic domain size. YAMAGUCHI and TOMITA (1970) have previously interpreted these facts as follow. Clinoenstatite occurring as an exsolution phase in the host diopside is a metastable phase which formed under the lattice distortion in the early stage during the process of exsolution of enstatite from the host diopside. In the later stage this metastable phase has grown to broad lamellae parallel to the (100) plane of the host diopside, so that they can be easily observed under the microscope. As the result of such growth, its lattice distortion was released, and the metastable clinoenstatite was converted into orthoenstatite as a stable phase. This interpretation can also be applied to the presence of clinoenstatite – clinohypersthene and orthoenstatite – hypersthene as (100) exsolution phases in Ca-rich pyroxene as shown in this study. The diallage partings in the crystals of C-7, C-8 and C-9 augites and the strongly mosaic crystalline textures of C-3 – C-6 diopsides confirmed by the asterisms of X-ray diffraction spots may be originated from the results of this release of lattice distortion.

2. Five clinopyroxene specimens more Fe-rich than Ca_{41} Mg_{41} -Fe_{18} enclose the (001) exsolution phases of clinopyroxene of pigeonite type. In three of them the exsolution and host phases indicate two-dimensional lattice distortion along their (001) boundary plane. However, in C-10 and C-14 augites they show one-dimensional lattice distortion along their *b*-axis. In C-12 augite specimen, in spite of its optical homogenuity under the microscope, the crystal has an exsolved clinopyroxene of pigeonite type with two-dimensional lattice distortion along their (001) plane in submicroscopic domain size.

BOWN and GAY (1960) have described that the exsolved pigeonite in the host augite from the Skaergaard intrusion have never inverted to hypersthene. It is noticed in the present study also that exsolved pigeonites have never been inverted to hypersthene. Furthermore C-11 and C-14 augites which coexist with Ca-poor orthopyroxenes in the host rocks enclose the exsolved clinopyroxene of pigeonite type rather than hypersthene. Since the host augites co-exist with orthopyroxenes in the host rocks, it is considered that these

exsolved clinopyroxenes have been crystallized in the host augites below the pigeonite – orthopyroxene inversion temperature. BINNS et al. (1963), BINNS (1965) and BOYD and BROWN (1968), from the chemical analyses of the (001) exsolution lamellae of this type in some augites, have pointed out their low Ca content in comparison with that of pigeonites (Fig. 8). Summarizing these results it is established that the (001) exsolution phases in the augite are clinohypersthene rather than pigeonites, and that they might have been crystallized in the host augite below the pigeonite – orthopyroxene inversion temperature.

From the results of detailed lattice analyses of these exsolved phases in this study, these facts may be explained as follow. Clinohypersthenes as exsolution phases have been crystallized under the lattice distortion, which in turn may have been originated from the maintenance of two-dimensional agreement not only in orientation but also in lattice dimension along their (001) boundary plane in the early stage during the process of exsolution. This lattice distortion may favor the crystallization of monoclinic form of hypersthene rather than orthorhombic form.

3. The chemical compositions of exsolved clinoenstatites – clinohypersthenes are shown in Fig. 8. In all Ca-rich clinopyroxenes from various kinds of igneous rocks, exsolved clinopyroxenes Fe-poorer than approximately Fs_{30} share the (100) plane with the host Ca-rich clinopyroxene, whereas the more Fe-rich members than Fs_{30} share the (001) plane with them. This point Fs_{30} is consistent with the inversion point at which Ca-poor pyroxene changes its crystal structure from orthorhombic to monoclinic in the process of fractionation of tholeiitic magma as observed in the Skaergaad intrusion (BROWN 1957), Stillwater complex (HESS 1960) and Hakone volcanics (KUNO 1950). But it is difficult to explain the change between the (100) and the (001) exsolution phases at the point Fs_{30} by the interpretation based on the pigeonite – orthopyroxene inversion. Therefore it is estimated that owing to the slight difference in lattice dimensions, the clinoenstatite – clinobronzite series pyroxenes Fe-poorer than Fs_{30} favor to share the (100) with the host, while clinohypersthene more Fe-rich than Fs_{30} tend to share the (001).

4. The (100) exsolution phases of twinned clinopyroxene in R-1, R-3 and R-4 orthopyroxenes show the apparent orthorhombic symmetry: i.e. their (102) plane is parallel to the (001) plane of the host orthopyroxene (Fig. 6). Furthermore it is noticed that the exsolved twinned clinopyroxenes in R-4 bronzite show two-dimensional lattice distortion, and those in R-1 and R-3 bronzites show one-dimensional lattice distortion. However, the (100) exsolution phase of clinopyroxene in R-2 bronzite shows neither such (100) twinning nor apparent orthorhombic symmetry as mentioned above, but it presents only

one-dimensional lattice distortion along the *b*-axis.

From these observations it is established that the degrees of lattice distortion of exsolved clinopyroxenes decreases in the following order; R-4 bronzite → R-1 and R-3 bronzites → R-2 bronzite. Thus, Ca-rich clinopyroxene as an exsolution phase may have been firstly crystallized as a twinned clinopyroxene with apparent orthorhombic symmetry under the two-dimensional lattice distortion, and thereafter it has grown to broad exsolution lamellae, accompanied by the decrease in the degree of lattice distortion and the disappearance of such (100) twinning.

These exsolved clinopyroxenes change their optical properties in correspondence with the order of the lattice distortion. The low birefringence and small extinction angle of narrow lamellae correspond to comparatively high order of lattice distortion and high birefringence and large extinction angle of broad lamellae as well as those of Ca-rich clinopyroxene correspond to low order of lattice distortion.

5. MORIMOTO and TOKONAMI (1969) have described the exsolved augite in pigeonite from Moore County meteorite, which shows two-dimensional lattice distortion. On the other hand, the exsolved augite in Koyama pigeonite (P-1 pigeonite in this study) shows one-dimensional lattice distortion, and the host pigeonite is going to be converted to orthohypersthene. Therefore it is concluded that Koyama pigeonite is of the later stage than Moore County pigeonite in the process of exsolution. Since the host phase in Koyama pigeonite shows extremely low Ca-content (Table 4), it belongs to clinohypersthene rather than pigeonite.

P-2 inverted pigeonite which coexists with P-1 pigeonite in the same rock does not show any crystallographic relation in orientation between the exsolution and the host phases. BROWN (1957) found the same fact in some inverted pigeonites from the Skaergaard intrusion. Therefore it may be considered that exsolved augite might have been firstly separated from the host pigeonite under the two-dimensional lattice distortion, and later have grown to the broad lamellae parallel to the (001) of host pigeonite and simultaneously the host pigeonite might have been changed to clinohypersthene by decreasing its Ca-content. Later the lattice distortion along the *a*-axis of each phase might be released, and the host clinohypersthene was inverted to orthohypersthene as a stable phase. After this inversion, the exsolved augite and the host hypersthene (after pigeonite) might have not any crystallographic relations in common, and the exsolved augite lamellae have grown to the irregular brebs or patches, resulting in the formation of myrmekitic intergrowth in hypersthene crystal.

CONCLUSION

Generally, exsolution phases of pyroxenes have been firstly formed with the decrease in solubility in subsolidus region with lowering temperatures under the one or two dimensional lattice distortion. The lattice distortion is originated by the maintenance of one- or two-dimensional agreement not only in orientation but also in lattice dimension along the boundary axis or plane of both the host and exsolved pyroxene phases.

The lattice distortion has a tendency to favor the formation of some metastable forms of exsolved pyroxene phase. Consequently, there occur minerals of clinoenstatite – clinoferrosilite series as the metastable exsolution phases in some host Ca-rich clinopyroxenes, and also in some cases, Ca-poor orthopyroxenes enclose the exsolution phase of Ca-rich twinned clinopyroxene with apparent orthorhombic symmetry. The validity of pyroxene exsolution phenomena as geologic thermometer is therefore lost.

When these exsolved metastable phases have grown to broad lamellae as seen in some cases, their lattice distortion is released, and they are disposed to convert into the stable form. Sometimes release of the lattice distortion in exsolved pyroxene phases have resulted in the formation of (100) diallage partings or strongly mosaic crystalline textures in some pyroxene crystals.

ACKNOWLEDGMENTS

The author wishes to express his hearty thanks to Prof. K. YAGI of the Hokkaido University, for his great interest and guidance in this work, and to Prof. T. UEDA, and Dr. K. TOMITA of Kyoto University, for their interest and valuable advice for this work. Dr. M. KOMATSU of Niigata University kindly analysed the chemical compositions of some pyroxene specimens and their exsolution lamellae by using EPMA. Specimens used in this work were kindly supplied by Prof. M. HUNAHASHI, Dr. M. OHTA and Mr. T. WATANABE of Hokkaido University, Dr. M. KOMATSU of Niigata University and Mr. M. NOCHI of the Civil Engineering Research Institute of Hokkaido Development Bureau. The author wishes to thank all these persons.

REFERENCES

BINNS, R.A., LONG, J.V.P. and REED, S.J.B., 1963. Some naturally occurring members of the clinoenstatite-clinoferrosilite mineral series. *Nature*, vol. 198, p. 777-778.

————, 1965. The mineralogy of metamorphosed basic rocks from the Willyama Complex, Broken Hill district, New South Wales. Part 2. Pyroxene, garnets, plagioclase, and opaque oxides. *Min. Mag.*, Vol. 35, p. 561-587.

BOWEN N.L. and SCHAIRER, J.F., 1935. The system MgO-FeO-SiO_2. *Amer. Jour. Sci.*, 5th ser., Vol. 29, p. 151-217.

BOWN, M.G. and GAY, P., 1959. The identification of oriented inclusions in pyroxene crystals. *Amer. Min.*, Vol. 44, p. 592-602.

————, ————, 1960. An X-ray study of exsolution phenomena in the Skaergaard pyroxenes. *Min. Mag.*, Vol. 32, p. 379-388.

BOWN, G.M., 1957. Pyroxenes from the early and middle stages of fractionation of the Skaergaard intrusion, east Greenland. *Min. Mag.*, Vol. 31, p. 511-543.

BÜKING, H., 1883. Bronzit vom Ultenthal (in Tyrol). *Zeits, Kryst. Min.*, 1883, Vol. 7, p. 502.

HARKER, A., 1909. The natural history of igneous rocks. Macmillan Co., New York. pp. 384.

HARKER, A., 1935. Petrology for students. Cambridge Univ. Press. pp. 283.

HESS, H.H., 1941. Pyroxenes of common mafic magmas, Part II. *Amer. Min.*, Vol. 26, p. 573-594.

————, 1949. Chemical composition and optical properties of common clinopyroxenes. *Amer. Min.*, Vol. 34, p. 621-666.

————, 1960. Stillwater igneous complex, Montana. Geol. Soc. Amer., Mem. 80, pp. 230.

KUNO, H., 1950. Petrology of Hakone volcano and the adjacent areas, Japan. *Bull. Geol. Soc. Amer.*, Vol. 61, p. 957-1019.

MORIMOTO N. and ITO T., 1958. Psendo-twin of augite and pigeonite. *Bull. Geol. Soc. Amer.*, Vol. 69. p. 1616.

————, and TOKONAMI, M., 1969. Oriented exsolution of augite in pigeonite. *Amer. Min.*, Vol. 54, p. 1101-1117.

NOCHI, M. and KOMATSU, M., 1967. Ultra basic rocks in the Hidaka metamorphic belt, Hokkaido, Japan II-Petrological relationships of the ultra basic rocks and the olivine gabbro in the Wensaru-Pankenushi area. *Earth Science*, Vol. 21, p. 11-26 (in Japanese).

POLDERVAART, A. and HESS, H.H., 1951. Pyroxenes in the crystallization of basaltic magma. *Journ. Geol.*, Vol. 59, p. 472-489.

VOGT, J.H.L., 1905. Physikalisch-Chemische Gesetze der Kristallisations-Folge in Eruptivgesteinen. *Tscherm. Min. Petr. Mitth.* (2), Vol. 24, p. 437-541.

YAMAGUCHI, Y. and TOMITA, K., 1958. On the exsolution lamellae of diopside in olivine gabbro from Horoman area Hokkaido. *Earth Science*, Vol. 22, p. 219-223 (in Japanese).

————, ————, 1970. Clinoenstatite as an exsolution phase in diopside. *Mem. Fac. Sci. Kyoto Univ.*, Vol. 37, no. 2, p. 174-180.

(Manuscript received July 27, 1972)

PLATES 1~6 AND EXPLANATION

Explanation of Plate 1

Fig. 1 (001) twin lamellae of C-1 diopside. ×100
Fig. 2 (001) twin lamellae of C-2 diopside. ×100
Fig. 3 (100) exsolution lamellae in C-5 diopside. ×200
Fig. 4 (100) exsolution lamellae in C-7 augite. ×100

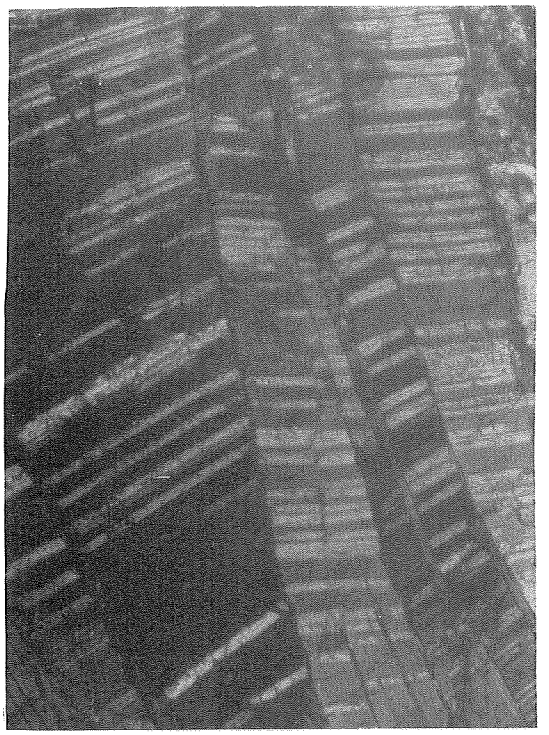

1

2

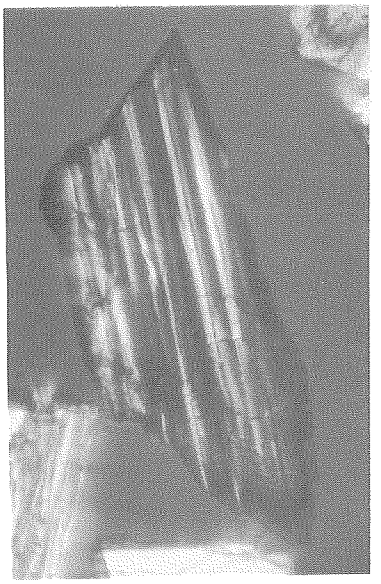

3

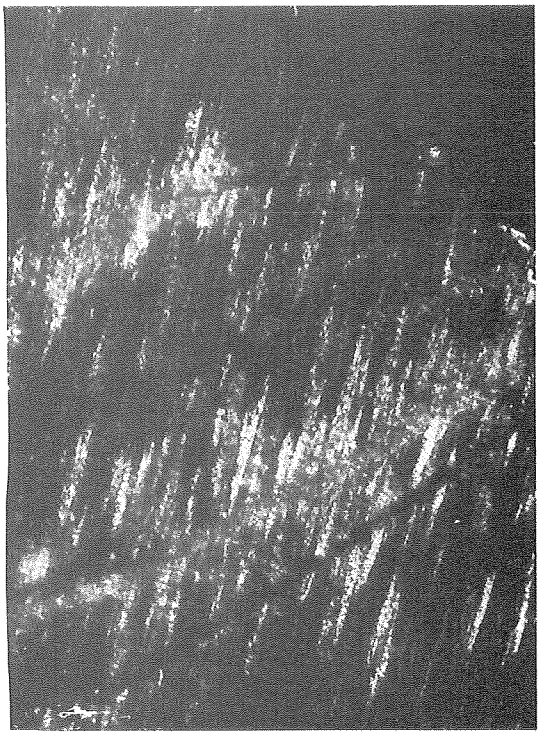

4

Explanation of Plate 2

Fig. 1 (100) exsolution lamellae in C-8 augite x100
Fig. 2 (001) exsolution lamellae in C-10 augite x300
Fig. 3 C-13 augite. x100
Fig. 4 (001) exsolution lamellae in C-14 ferroaugite. x100

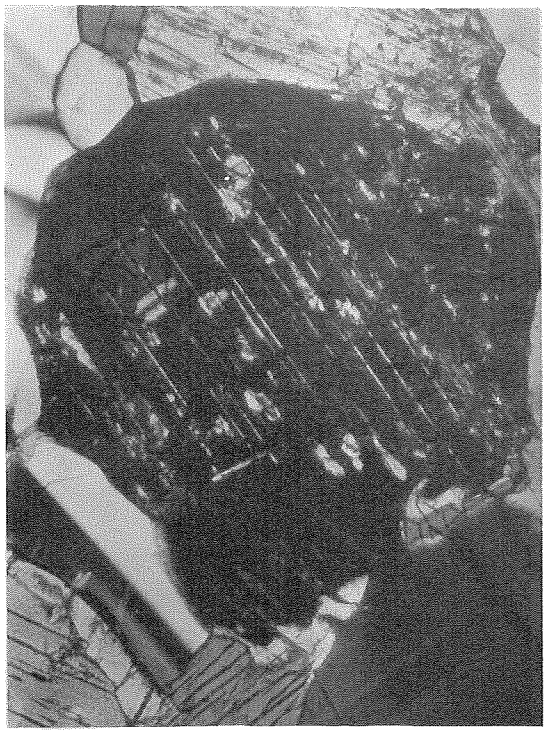

1

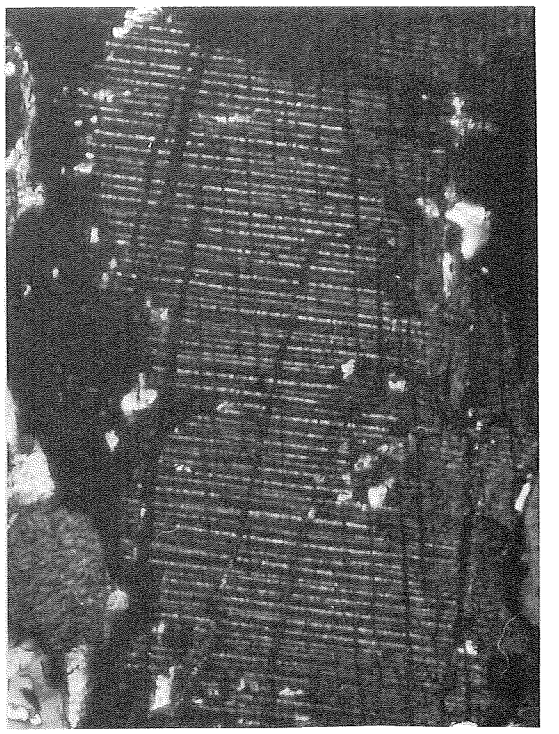

2

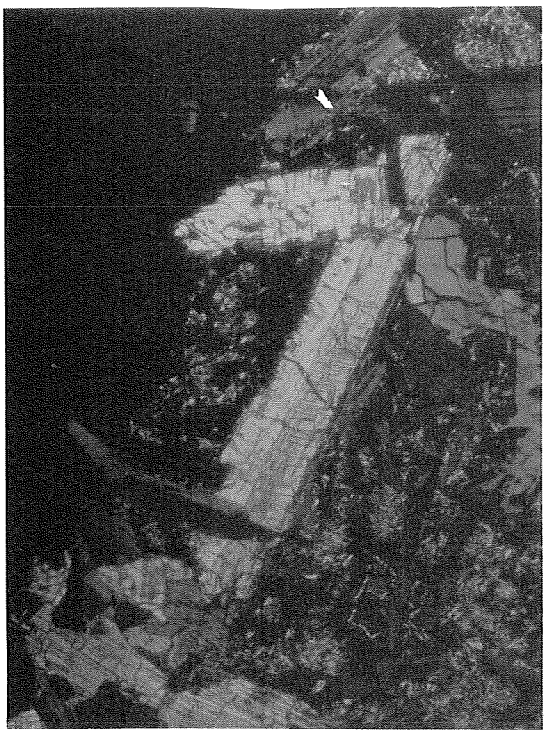

3

4

Explanation of Plate 3

Fig. 1 (100) exsolution lamellae in R-1 bronzite. x100

Fig. 2 (100) exsolution lamellae in R-2 bronzite. x100

Fig. 3 (001) exsolution lamellae in P-1 pigeonite.
P; pigeonite H; hypersthene x200

Fig. 4 Exsolution lamellae parallel to the (001) of the original pigeonite in P-2 inverted pigeonite. x250

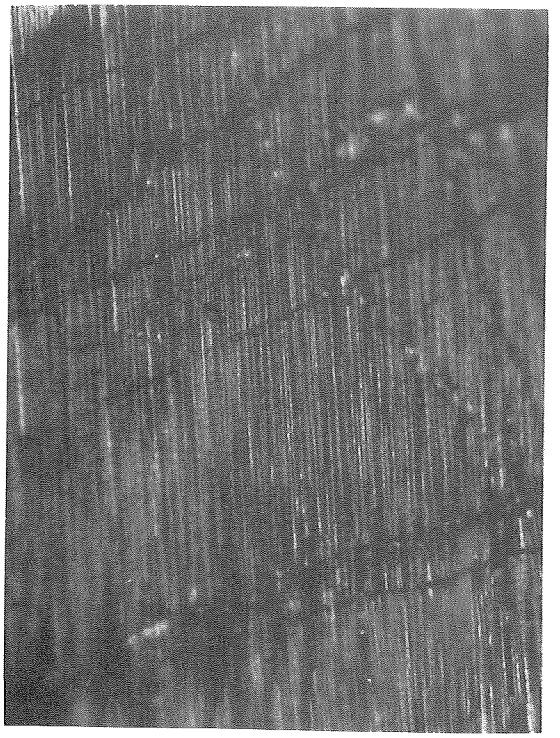

1

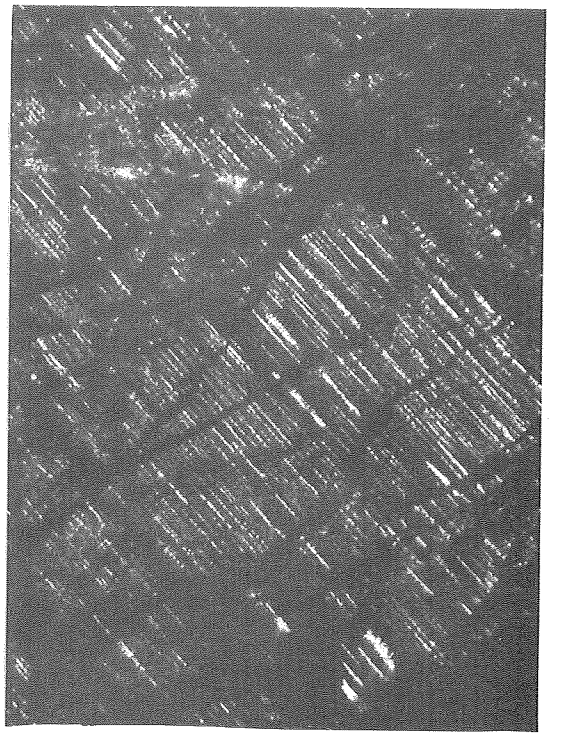

2

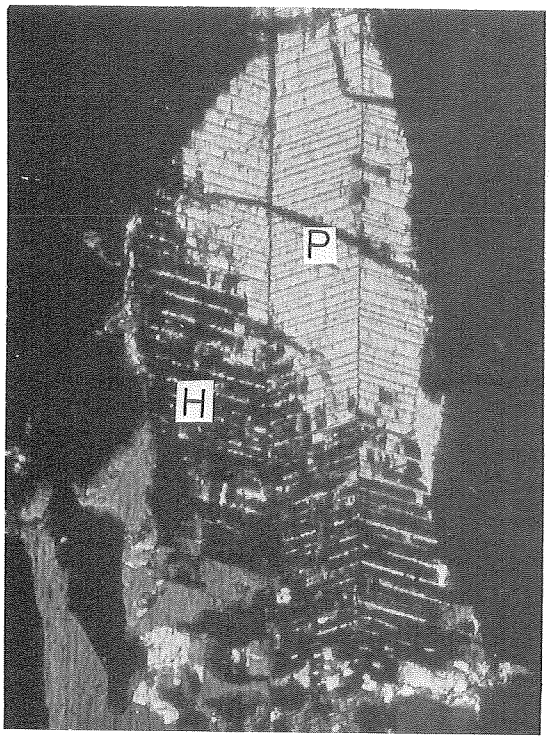

3

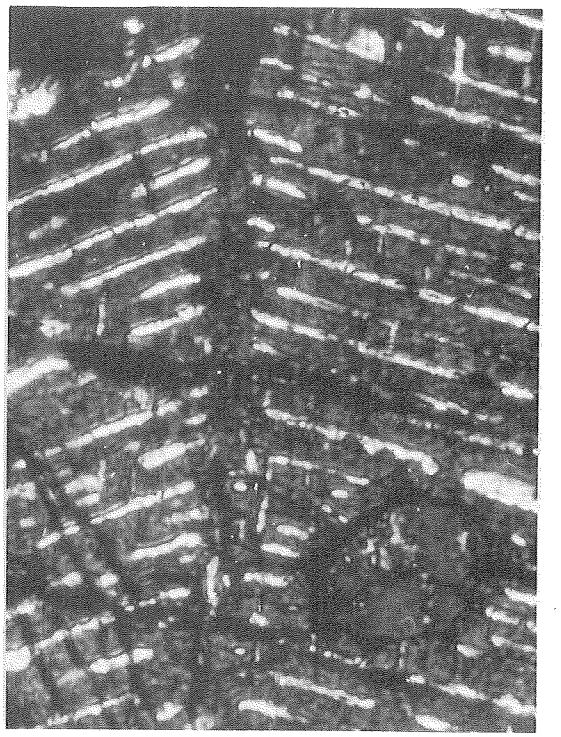

4

Explanation of Plate 4

Fig. 1 Laue photograph (b-axis) of C-3 diopside.
Fig. 2 h01* precession photograph of C-3 diopside.
Fig. 3 h01* precession photograph of the crystal without exsolution lamellae in C-5 diopside.
Fig. 4 h01* precession photograph of C-10 augite

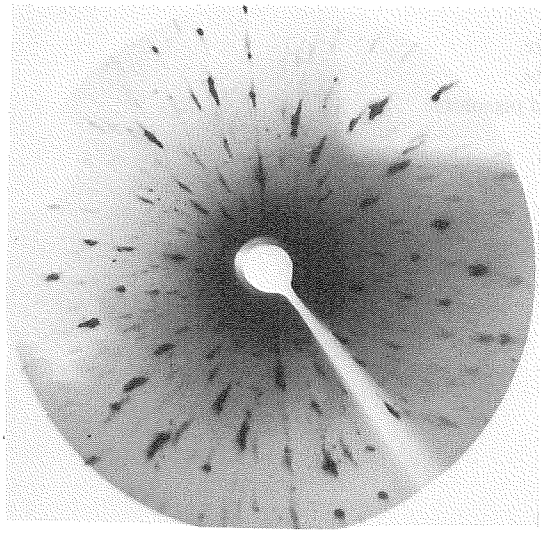

1

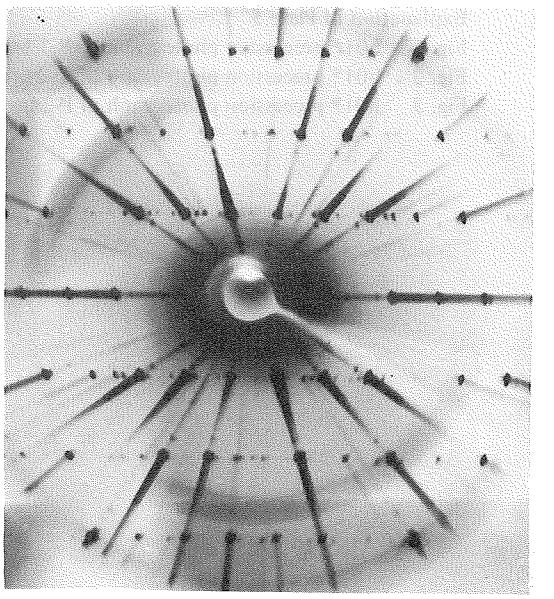

2

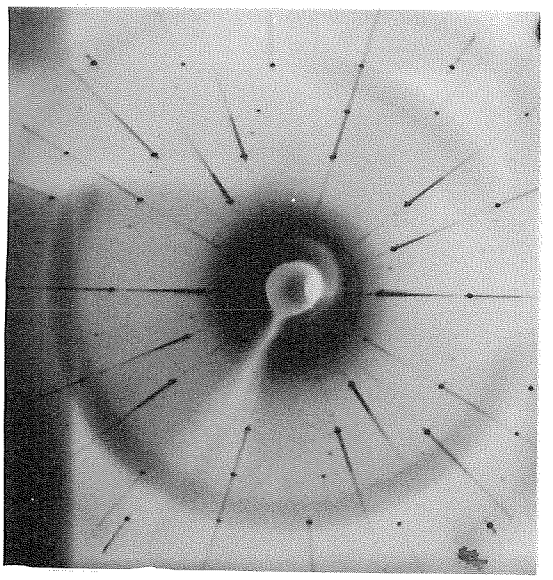

3

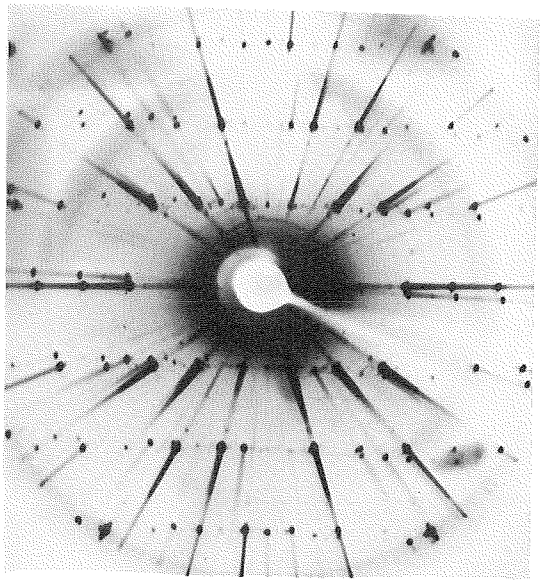

4

Explanation of Plate 5

Fig. 1 h01* precession photograph of R-1 bronzite.

Fig. 2 h01* precession photograph of R-2 bronzite.

Fig. 3 h01* precession photograph of P-2 inverted pigeonite.

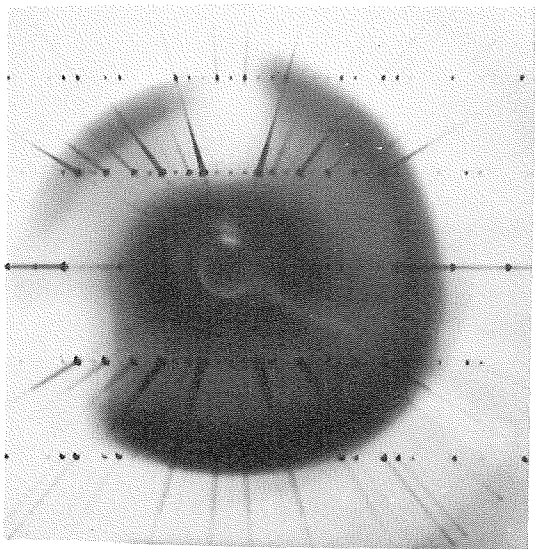

1

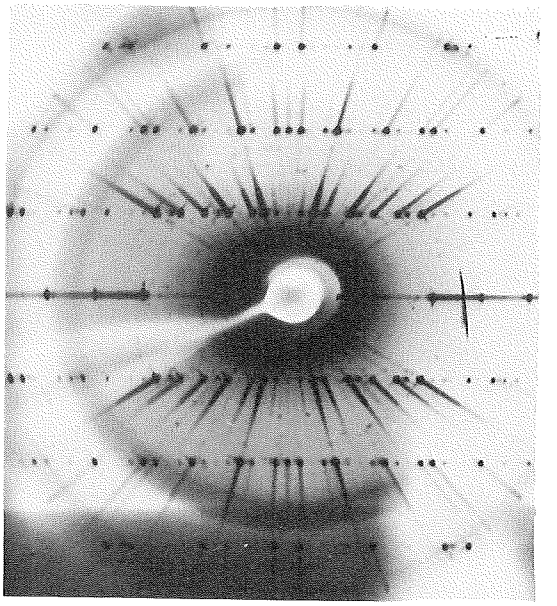

3

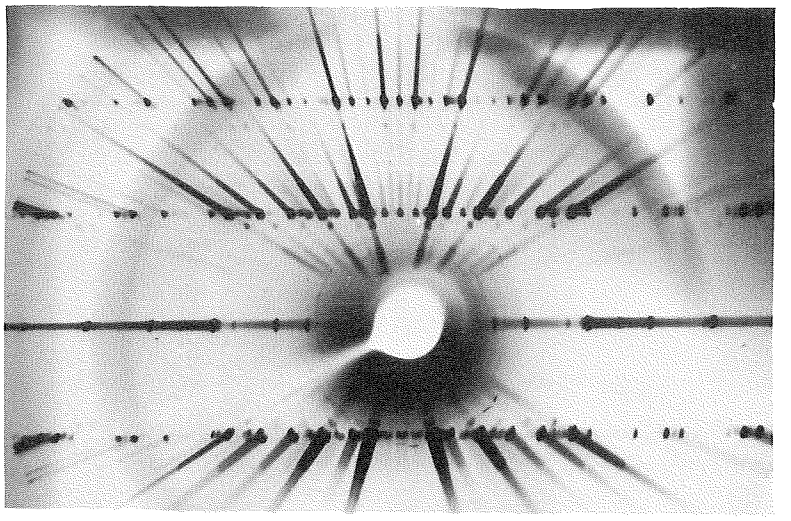

2